Numerically stable secular equation for superlattices via transfer-matrix formalism and application to $InAs/In_{0.23}Ga_{0.77}Sb$ and $InAs/In_{0.3}Ga_{0.7}Sb/GaSb$ superlattices

Frank Szmulowicz*
Wright Laboratory, Materials Directorate, WL/MLPO, Wright-Patterson AFB, Ohio 45433-7707
(Received 22 July 1997; revised manuscript received 3 November 1997)

The numerically stable, Hermitian secular equation for superlattices within the envelope-function approximation [F. Szmulowicz, Phys. Rev. B **54**, 11 539 (1996)] is derived via the transfer-matrix approach using Burt's boundary conditions. In the process, the tangents-only form of the secular equation is related to an earlier transfer matrix approach [L. R. Ram-Mohan, K. H. Yoo, and R. L. Aggarwal, Phys. Rev. B **38**, 6151 (1988)] and extended to structures with an arbitrary number of layers per superlattice period. The formalism is applied to superlattices with two ($InAs/In_{0.23}Ga_{0.77}Sb$) and three ($InAs/In_{0.3}Ga_{0.7}Sb/GaSb$) layers per superlattice period, which are of interest for infrared detector and infrared cascade-laser applications, respectively. [S0163-1829(98)03015-X]

I. INTRODUCTION

The envelope-function approximation (EFA) for calculating the electronic structure of quantum dots, wires, wells, and superlattices[1] continues to be popular because of its immediate physical appeal, being ''an extremely concise representation of heterostructure electronic properties... [with] the computational effort essentially independent of the number of atoms in the system.'' [2] There is active research in exploring[2,3] and overcoming[4,5] the physical limitations of the EFA theory. For example, Wood and Zunger[2] showed that for an accurate description of GaAs/AlAs superlattices (SL's) via the EFA, the associated $\mathbf{k}\cdot\mathbf{p}$ bulk bands must be well described, which requires about 30 bands at the zone center.

Increasing the number of bands in the EFA formalism can accentuate a number of numerical stability problems, including the occurrence of large exponentials due to the presence of large, imaginary, spurious exponents.[6–8] The recently derived secular equation for superlattices in the EFA formalism[8] can successfully handle a large number of bands. It does not require that the bulk $\mathbf{k}\cdot\mathbf{p}$ Hamiltonian be first block diagonalized to eliminate the Kramers' degeneracy, a difficult enough procedure for the six- and eight-band EFA.[9] The resulting secular equation is Hermitian, so that its eigenvalues are real.[8] Because of its tangent form, the secular equation is numerically stable with respect to the occurrence of large exponentials, because for large arguments, the tangents become hyperbolic tangents which are bounded by ± 1. Since the derivation in Ref. 8 was pursued via a special trigonometric approach, its relationship to the earlier transfer-matrix formalism of Ram-Mohan, Yoo, and Aggarwal[6] (RYA) approach is unclear.

In this paper, the secular equation of Ref. 8 is derived through the transfer-matrix approach using Burt's boundary conditions.[4] The technique used to derive the secular equation is then applied to obtain numerically stable forms for the calculation of the electronic properties of superlattices with an arbitrary number of layers per superlattice period. Section II establishes the notation and develops the transfer-matrix formalism using the present (SZ) and RYA approaches. A Kronig-Penney-like equation is derived for SL's with an arbitrary number of layers per superlattice period. In Sec. III, the transfer-matrix formalism is used to derive the tangents-only form of the secular equation from Ref. 8. The tangents-only form is then derived for an arbitrary number of layers per superlattice period. The formalism is applied in Sec. IV to $InAs/In_{0.23}Ga_{0.77}Sb$ and $InAs/In_{0.3}Ga_{0.7}Sb/GaSb$ superlattices, where their electronic structures are calculated and the optical absorption spectrum of $InAs/In_{0.23}Ga_{0.77}Sb$ is shown. Conclusions are presented last.

II. TRANSFER-MATRIX FORMALISM FOR COUPLED-BAND EFA

A. Notation

Consider a superlattice (SL) consisting of alternating layers of material A of width $2a$ and material B of width $2b$. In the zeroth unit cell, material A ranges between $(b<z\leqslant b+2a)$ and material B between $(-b<z\leqslant b)$. The period is $w=2a+2b$. For the N-coupled band EFA formalism,[1,4–9] the envelope function for a superlattice miniband M is an N-component vector $F(M,\mathbf{k}_\parallel q,z)$ with components $F_\nu(M,\mathbf{k}_\parallel,q,z)$, $\nu=1,...,N$, where $(\mathbf{k}_\parallel,q)$ are wave vectors in the SL layer plane and in the growth direction, respectively. The N-component envelope function satisfies the Bloch periodicity condition

$$F_\nu(M,\mathbf{k}_\parallel q,z+w)=e^{iqw}F_\nu(M,\mathbf{k}_\parallel q,z). \tag{1}$$

The EFA theory uses the bulk $\mathbf{k}\cdot\mathbf{p}$ Hamiltonian $H(\mathbf{k}_\parallel,k_z)$ of order $N\times N$ for the constituent materials of the heterostructure. Expanded to second order, the EFA Hamiltonian becomes[4]

$$H(\mathbf{k}_\parallel,k_z)=k_zH_2(\mathbf{k}_\parallel)k_z+\frac{1}{2}\left[H_{1R}(\mathbf{k}_\parallel)k_z+k_zH_{1L}(\mathbf{k}_\parallel)\right]+H_0(\mathbf{k}_\parallel), \tag{2}$$

where the operator $k_z=-id/dz$. In Burt's formalism,[4] $[H_{1L}]^{\dagger}=H_{1R}$. Away from interfaces, define $[H_{IL}+H_{1R}]/2 \equiv H_1$. Matrices $H_0(\mathbf{k}_{\|})$, $H_1(\mathbf{k}_{\|})$, and $H_2(\mathbf{k}_{\|})$ are Hermitian and material specific (z dependent).[7]

Away from interfaces, in each layer of the heterostructure, the EFA Schrödinger equation reads

$$H_2\frac{d^2F}{dz^2}+iH_1\frac{dF}{dz}-(H_0-E)F=0, \tag{3}$$

or

$$\frac{d^2F}{dz^2}+i(H_2)^{-1}H_1\frac{dF}{dz}-(H_2)^{-1}(H_0-E)F=0. \tag{4}$$

Changing the second-order Schrödinger equation into a first-order equation doubles the length of the eigenvector, yielding the EFA equation[6]

$$i\Omega(z)f(z)=\frac{df(z)}{dz}, \tag{5}$$

where Ω is of order $2N\times 2N$. The forms chosen here (SZ) and by RYA are as follows:

$$i\Omega_{\mathrm{SZ}}=\begin{pmatrix} 0 & I \\ H_2^{-1}(H_0-E) & -iH_2^{-1}H_1 \end{pmatrix}, \quad f_{\mathrm{SZ}}=\begin{pmatrix} F \\ F' \end{pmatrix}, \tag{6a}$$

$$i\Omega_{\mathrm{RYA}}=\begin{pmatrix} -iH_2^{-1}H_1/2 & H_2^{-1} \\ (H_0-E)-H_1H_2^{-1}H_1/4 & -iH_1H_2^{-1}/2 \end{pmatrix},$$

$$f_{\mathrm{RYA}}=\begin{pmatrix} F \\ H_2F'+iH_1F/2 \end{pmatrix}. \tag{6b}$$

While the second rows of Eqs. (6) contain the Schrödinger equation itself, the first row reduces to a simple identity $F'=F'$. The two formalism can be shown to be related via a similarity transformation.[10]

In regions of constant composition, Ω is constant, so that the formal solution of Eq. (5) is[6]

$$f(z)=e^{i\Omega z}f(0)\equiv T(z)f(0), \tag{7}$$

where $f(0)$ is a constant of integration and $T(z)\equiv e^{i\Omega z}$ is the transfer matrix, which is evaluated by first diagonalizing Ω. Let matrix P diagonalize matrix Ω,

$$P^{-1}\Omega P=K, \tag{8}$$

where K is diagonal, $K_{ij}=k_i\delta_{ij}$, $i=1,...,2N$, which defines a set of exponents $\{k\}$, so that

$$e^{i\Omega z}=Pe^{iKz}P^{-1}, \tag{9}$$

where

$$(e^{iKz})_{ij}=e^{ik_iz}\delta_{ij}. \tag{10}$$

Because the two formalisms are related by a similarity transformation,[10] exponents $\{k\}$ in both formalisms are the same, but the associated eigenvectors, which are stored as the columns of matrix $P(\Omega P_i=k_iP_i)$, are not. Exponents $\{k\}$ are the roots of the following determinental equation, which leads to the same characteristic polynomial in k for both formalisms,

$$\|\Omega_{\mathrm{SZ}}-k\|=\|\Omega_{\mathrm{RYA}}-k\| =\|H_2k^2+H_1k+(H_0-E)\|=0, \tag{11}$$

which is equivalent to the starting $\mathbf{k}\cdot\mathbf{p}$ Hamiltonian, Eq. (2). If vector C is the right eigenvector[7] of $(H_2k^2+H_1k+H_0)C=EC$, then $P=\binom{C}{KC}$, which establishes the correspondence with Eq. (22) of Ref. 8. Using Eqs. (7)–(10), the upper half of vector $f(z)$ has the form

$$F_\nu(z)=\sum_{i=1}^{2N}C_{\nu i}\exp(ik_iz)c_i, \tag{12}$$

[see Eq. (19) of Ref. 8] where

$$c_i=\sum_{\mu=1}^{2N}P_{i\mu}^{-1}f_\mu(0). \tag{13}$$

B. Boundary conditions

Burt[4] developed an exact EFA that avoids *ad hoc* assumptions about the boundary conditions. In practical implementations of Burt's formalism (see, for example, Foreman[5]), the effective-mass equation for the single and coupled-band cases has the form of a differential equation with piecewise-constant coefficients. As implemented by Foreman, the boundary conditions require the continuity of the envelope function F and of the quantity $H_2F'+(iH_{1L}/2)F$, which is obtained by integrating the Schrödinger equation across an interface. Equivalently, we require the continuity of

$$\begin{pmatrix} I & 0 \\ iH_{1L}/2 & H_2 \end{pmatrix}\begin{pmatrix} F \\ F' \end{pmatrix}=S_{\mathrm{SZ}}f_{\mathrm{SZ}}. \tag{14a}$$

In the standard EFA, $H_1=H_{1L}$, so that in the RYA approach, f_{RYA} itself is continuous across an interface.[6] However, with Burt's boundary conditions, the RYA approach requires the continuity of

$$\begin{pmatrix} I & 0 \\ i(H_{1L}-H_{1R})/4 & I \end{pmatrix}\begin{pmatrix} F \\ H_2F'+iH_1F/2 \end{pmatrix}\equiv S_{\mathrm{RYA}}f_{\mathrm{RYA}}. \tag{14b}$$

Therefore, with Burt's boundary conditions, it is functionally simpler (FS) to use

$$i\Omega_{\mathrm{FS}}=\begin{pmatrix} -iH_2^{-1}H_{1L}/2 & H_2^{-1} \\ (H_0-E)-H_1H_2^{-1}H_{1L}/4 & -iH_{1R}H_2^{-1}/2 \end{pmatrix},$$

$$f_{\mathrm{FS}}=\begin{pmatrix} F \\ H_2F'+iH_{1L}F/2 \end{pmatrix}, \tag{14c}$$

for which f_{FS} is continuous at each interface and $S_{\mathrm{FS}}=I$.

C. Transfer-matrix equations

In what follows, subscripts SZ, RYA, and FS are dropped. Integrating Eq. (5) across one period from $-b$ to $b+2a$, one finds

$$f_A(2a+b)=e^{i2\Omega_A a}f_A(b)=e^{i2\Omega_A a}S_A^{-1}S_B e^{i2\Omega_B b}f_B(-b)$$
$$=e^{iqw}S_A^{-1}S_B f_B(-b), \tag{15}$$

where $f_{A,B}, S_{A,B}$ stand for quantities evaluated at the A,B side of a particular interface and the last equality employs the Bloch theorem. This leads to the common secular equation for all three (SZ, RYA, FS) cases,

$$[(S_A e^{i2\Omega_A a}S_A^{-1})(S_B e^{i2\Omega_B b}S_B^{-1})-e^{iqw}]S_B f_B(-b)=0. \tag{16}$$

Define matrix M as

$$Se^{i\Omega z}S^{-1}=(SP)e^{iKz}(SP)^{-1}\equiv Me^{iKz}M^{-1}, \tag{17}$$

where

$$M\equiv SP. \tag{18}$$

Thus defined, matrix M is the same as Eq. (22) of Ref. 8. Equation 17 can be used to define the final exponential matrix,

$$e^{i\Lambda z}\equiv Me^{iKz}M^{-1}, \tag{19}$$

so that the secular equation, Eq. (16), becomes

$$[e^{i2\Lambda_A a}e^{i2\Lambda_B b}-e^{iqw}]S_B f_B(-b)=0, \tag{20}$$

in which the unknowns are the energy and vector $S_B f_B(-b)$.

The nontrivial solution of Eq. (20) requires that the secular determinant be zero,

$$\|e^{i2\Lambda_A a}e^{i2\Lambda_B b}-e^{iqw}\|=0. \tag{21}$$

The time-reversal symmetry allows us to write this equation as

$$\|I-e^{iqw}e^{i2\Lambda_A a}e^{i2\Lambda_B b}\|=0. \tag{22}$$

Integrating Eq. 5 from $b+2a$ to $-b$, one finds an equivalent secular equation,

$$f_B(-b)=e^{-i2\Omega_B b}f_B(b)$$
$$=e^{-i2\Omega_B b}S_B^{-1}S_A e^{-i2\Omega_A a}S_A^{-1}S_B f_B(b+2a)$$
$$=e^{-iqw}f_B(b+2a), \tag{23}$$

or

$$[(S_B e^{-i2\Omega_B b}S_B^{-1})(S_A e^{-i2\Omega_A a}S_A^{-1})-e^{-iqw}]S_B f_B(b+2a)$$
$$=0, \tag{24}$$

which requires that

$$\|e^{-i2\Lambda_B b}e^{-i2\Lambda_A a}-e^{-iqw}\|=0. \tag{25}$$

Multiplying Eq. (22) and Eq. (25) together, one finds a Kronig-Penney-like equation,

$$\left\|\frac{e^{i2\Lambda_A a}e^{i2\Lambda_B b}+e^{-i2\Lambda_B b}e^{-i2\Lambda_A a}}{2}-\cos\, qw\right\|=0. \tag{26}$$

In the one-band limit, Eq. (26) is diagonal with the Kronig-Penney equation twice on the diagonal. Generalizing to M layers per superlattice period, one finds[11]

$$\left\|\frac{e^{i2\Lambda_A a}e^{i2\Lambda_B b}\cdots e^{i2\Lambda_M m}+e^{-i2\Lambda_M m}\cdots e^{-i2\Lambda_B b}e^{-i2\Lambda_A a}}{2}\right.$$
$$\left.-\cos\, qw\right\|=0. \tag{27}$$

III. TANGENTS-ONLY FORM

A. Derivation

Consider Eq. (24),

$$[e^{-i2\Lambda_B b}e^{-i2\Lambda_A a}-e^{-iqw}]S_B f_B(b+2a)$$
$$=[e^{-i2\Lambda_B b}e^{-i2(\Lambda_A a-qw/2)}-I]S_B f_B(-b)=0, \tag{28}$$

where one of several ways of factoring out $\exp(-iqw)$ is used. Using the operator identity[12]

$$e^{-i2\Lambda a}=\frac{1-i\,\tan\Lambda a}{1+i\,\tan\Lambda a}=(1+i\,\tan\Lambda a)^{-1}(1-i\,\tan\Lambda a), \tag{29}$$

Eq. (28) can be rewritten as

$$\left\{\left[\frac{1-i\,\tan(\Lambda_B b)}{1+i\,\tan(\Lambda_B b)}\right]\left[\frac{1-i\,\tan(\Lambda_A a-qw/2)}{1+i\,\tan(\Lambda_A a-qw/2)}\right]-I\right\}S_B f_B(-b)$$
$$=0. \tag{30}$$

To remove the denominators, multiply Eq. (30) on the left by $(1+i\,\tan\Lambda_B b)$ and insert the unit matrix $I=[1+i\,\tan(\Lambda_A a-qw/2)][1+i\,\tan(\Lambda_A a-qw/2)]^{-1}$ after the curly brackets, which results in

$$[\tan(\Lambda_B b)+\tan(\Lambda_A a-qw/2)]X=0, \tag{31}$$

where

$$X=\cos(\Lambda_A a-qw/2)e^{-i(\Lambda_A a-qw/2)}S_B f_B(-b), \tag{32}$$

which can be used to find $f_B(-b)$ and then the rest of the envelope function. This equation corresponds to Eq. (36) of Ref. 8. Equation (20) also leads to Eq. (31), but with

$$X=\cos\,\Lambda_B b e^{i\Lambda_B b}S_B f_B(-b), \tag{33}$$

which corresponds to Eq. (37) of Ref. 8.

This new system of equations has a nontrivial solution when[13]

$$\|\tan(\Lambda_A a-qw/2)+\tan(\Lambda_B b)\|=0; \tag{34}$$

other equivalent forms are obtained by different ways of factoring the exponential in Eq. (28), for example,

$$\|\tan(\Lambda_A a)+\tan(\Lambda_B b-qw/2)\|=0, \tag{35}$$

or the most symmetric form,

$$\|\tan(\Lambda_A a-qw/4)+\tan(\Lambda_B b-qw/4)\|=0. \tag{36}$$

Of course, in order to evaluate any of the tangents one must know the matrix diagonalizing its argument, so that, for example, from Eq. (34),

$$\|M_B\,\tan(K_B b)M_B^{-1}+M_A\,\tan(K_A a-qw/2)M_A^{-1}\|=0. \tag{37}$$

Equations (31)–(37) represent the central results of the present paper.

B. Multiple layers per period

For concreteness, consider a three-layer superlattice with layers A $(0<z\leqslant 2a)$, B $[2a<z\leqslant 2(a+b)]$, and $C[2(a+b)<z\leqslant 2(a+b+c)]$. Integrating the first-order differential equation across each individual layer, one obtains

$$f_A(2a)=e^{i2\Omega_A a}f_A(0), \tag{38a}$$

$$f_B(2a+2b)=e^{i2\Omega_B b}f_B(2a), \tag{38b}$$

$$f_C(2a+2b+2c)=e^{i2\Omega_C c}f_A(2a+2b). \tag{38c}$$

The boundary conditions across the interfaces provide the following equations

$$S_A[e^{i2\Omega_A a}f_A(0)]=S_B f_B(2a), \tag{39a}$$

$$S_B[e^{i2\Omega_B b}f_B(2a)]=S_C f_C(2a+2b), \tag{39b}$$

$$S_C[e^{i2\Omega_C c}f_C(2a+2b)]=e^{iqw}S_A f_A(0), \tag{39c}$$

where the last line employs the Bloch periodicity conditions. Besides the energy, there are three unknowns in the problem: $f_A(0)$, $f_B(2a)$, and $f_C(2a+2b)$. The boundary conditions can be arranged in a 3×3 matrix, in which each element is a $2N\times 2N$ matrix itself:

$$\begin{pmatrix} \exp(2i\Lambda_A a) & -I & 0 \\ 0 & \exp(2i\Lambda_B b) & -I \\ -I & 0 & \exp[2i(\Lambda_C c-qw/2)] \end{pmatrix} \times \begin{pmatrix} S_A f_A(0) \\ S_B f_B(2a) \\ S_C f_C(2a+2b) \end{pmatrix} = 0. \tag{40}$$

The secular equation can be reduced to a $2N\times 2N$ equation in one unknown, say $f_A(0)$, at the price of retaining the potentially troublesome exponentials [see, for example, Eq. (24) for two layers and Eq. (27) for multiple layers]. Equation 40 has a clearly discernible pattern that can be extended to more than three layers.

To eliminate the exponentials in Eq. (40), however, use the half-angle formula, Eq. (29), which makes it possible to transform the secular equation into

$$\begin{pmatrix} \tan\Lambda_A a & iI & -iI \\ -iI & \tan\Lambda_B b & iI \\ iI & -iI & \tan(\Lambda_C c-qw/2) \end{pmatrix} \begin{pmatrix} (1-i\tan\Lambda_A a)^{-1}S_A f_A(0) \\ (1-i\tan\Lambda_B b)^{-1}S_B f_B(2a) \\ [1-i\tan(\Lambda_C c-qw/2)]^{-1}S_C f_C(2a+2b) \end{pmatrix} = 0 \tag{41}$$

and the eigenvalue condition is

$$\begin{Vmatrix} \tan\Lambda_A a & iI & -iI \\ -iI & \tan\Lambda_B b & iI \\ iI & -iI & \tan(\Lambda_C c-qw/2) \end{Vmatrix} = 0. \tag{42}$$

Setting the thickness of any one layer to zero leads to the two-layer result, Eq. (34).

Here, the price for avoiding the uncontrollable growth of the exponentials is an increase in the size of the secular matrix. However, one gains in numerical stability. Another benefit is that Eq. (41) can be made Hermitian, so that in the diagonalization of Eq. (42), the diagonal elements are real and come in Kramers' degenerate pairs. At an eigenvalue, two of the diagonals are zero and the two associated eigenvectors contain $f_A(0)$, $f_B(2a)$, and $f_C(2a+2b)$ for the Kramers' degenerate superlattice miniband.

Equation (42) establishes the pattern for odd number of layers per superlattice period: the tangent matrices for each layer are on the diagonals; above the diagonal, the ijth element is the $2N\times 2N$ unit matrix times $i(-1)^{i+j+1}$; and below the diagonal, the matrix is the Hermitian conjugate of the matrix above the diagonal.

For even numbers of layers, the pattern for the secular matrix is clear from the following four-layer result for layers A, B, C, and D (widths $2a$, $2b$, $2c$, and $2d$, respectively):

$$\begin{Vmatrix} \tan\Lambda_A a & \tan\Lambda_B b & iI & -iI \\ -iI & \tan\Lambda_B b & \tan\Lambda_C c & iI \\ iI & -iI & \tan\Lambda_C c & \tan(\Lambda_D d-qw/2) \\ \tan\Lambda_A a & iI & -iI & \tan(\Lambda_D d-qw/2) \end{Vmatrix} = 0. \tag{43}$$

Alternately, the four-layer result can be obtained from the five-layer result, with one of the layers having zero thickness,

$$\begin{Vmatrix} \tan\Lambda_A a & iI & -iI & iI & -iI \\ -iI & \tan\Lambda_B b & iI & -iI & iI \\ iI & -iI & \tan\Lambda_C c & iI & -iI \\ -iI & iI & -iI & \tan(\Lambda_D d-qw/2) & iI \\ iI & -iI & iI & -iI & 0 \end{Vmatrix} = 0, \tag{44}$$

where the last row leads to a redundant equation.

Once the roots of the determinental equation are found by diagonalizing the secular equation, the eigenvectors corresponding to the zero diagonals can be used to solve for the envelope function via the transfer equation, Eq. (7). For example, for three layers, Eq. (41) can be used to find $S_A f_A(0)$, $S_B f_B(2a)$, and $S_C f_C(2a+2b)$, which provide the required initial values to produce the wave function at any z via Eq. (7). For example, in layer A,

$$F_v(z)=\sum_{i=1}^{2N}(M_A)_{vi}\exp(ik_i z)\alpha_i, \tag{45a}$$

where

$$\alpha_i=\sum_{\mu=1}^{2N}(M_A^{-1})_{i\mu}[S_A f_A(0)]_\mu. \tag{45b}$$

C. Hermiticity

The theory development in Ref. 8 concentrates in greater detail on the various ingredients that go into the construction of the secular equation. In particular, from the analytic properties of the M matrix, Eq. (18), it was shown in Ref. 8 that the secular determinants in Eqs. (26), (27), and (34)–(37) (which are of order $2N\times 2N$) can be rendered Hermitian by interchanging their first and last N rows (or columns), which greatly simplifies the subsequent analysis, particularly, the location of the zeroes of the secular determinant.

For more than two layers per superlattice period, the secular matrix in Eqs. (41), (42), and (44) [but not Eq. (43)] can be rendered Hermitian if the first N rows/columns are interchanged with the second N rows/columns and then similarly for the third with the fourth, the fifth with the sixth, etc. The proof follows the lines of Ref. 8.

IV. APPLICATIONS

A. InAs/$In_{0.23}Ga_{0.77}Sb$ superlattice

The InAs/$In_{0.23}Ga_{0.77}Sb$ superlattice is of interest for infrared detector applications.[7,8,14,15] The superlattice used as an example here is designed to operate as an infrared detector with a 10-μm long-wavelength cutoff. The $In_xGa_{1-x}Sb$ layer is 17.3 Å wide with $x=0.23$ indium mole fraction and the InAs layer is 43.6 Å wide. The structure is strained to a GaSb substrate oriented in the [001] direction, and the InAs conduction band–GaSb valence-band overlap is taken to be 140 meV. The band gap in this structure is tailored to be 120 meV and the layer widths were chosen to yield maximum absorption with respect to variations in their widths. The zero of energy is placed at the bottom of the conduction band of unstrained bulk InAs. Using the material parameters from Ref. 15, the electronic structure and the optical absorption coefficients are calculated using the formalism developed in this paper in conjunction with the 8×8 EFA Hamiltonian and the standard EFA boundary conditions.[8] First, the eigenergies are obtained using Eq. (34) and then the wave functions are found using Eq. (32). These wave functions are then used to find the optical matrix elements ($\mathbf{k}_\parallel$ dependent) by an extension[16] of the formalism first derived by Chang and James.[17] Lastly, the optical spectrum is calculated, with the necessary Brillouin zone integration performed with the Gilat-Raubenheimer scheme.[18] Because of the tangent form of Eq. (34), the secular determinant was on the order of unity and its roots could be easily located by multiplying the distinct eigenvalues of the secular matrix, which was first rendered Hermitian by row interchange. By contrast, the exponential form of the secular equation, Eq. (26), involves exponentials on the order of $10^{\pm 103}$ (spurious imaginary exponent of 2.36 (1/Å) times InAs width of 43.6 Å = 103), which makes root search impossible. The wave functions were easily found, normalized, and then used for the calculation of the optical oscillator strengths.

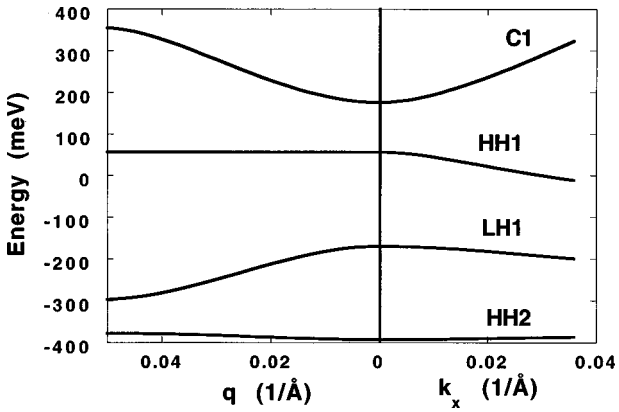

FIG. 1. The band diagram for the 43.6/17.3 Å InAs/$In_{0.23}Ga_{0.77}Sb$ superlattice.

Using Eq. (34), the band dispersions for the superlattice were calculated, Fig. 1, which shows three main bands—LH1, HH1, and $C1$, where LH, HH, and C are light hole, heavy hole, and conduction, respectively. The corresponding optical absorption in normal incidence is shown in Fig. 2, showing absorption comparable to $Hg_xCd_{1-x}Te$ detectors operating in the same wavelength range.[14] For light polarized in the z direction, Fig. 3, the near-threshold absorption is lower than for normal incidence, but it is a little appreciated point that the two become comparable at higher energies. Atomic selection rules on the Bloch parts of the total wave functions allow HH1 to $C1$ and LH1 to $C1$ transitions in normal incidence and LH1 to $C1$ in z polarization at the center of the Brillouin zone. However, HH1 to $C1$ absorption in z polarization is forbidden and only becomes allowed away from the Brillouin-zone center because of band mixing

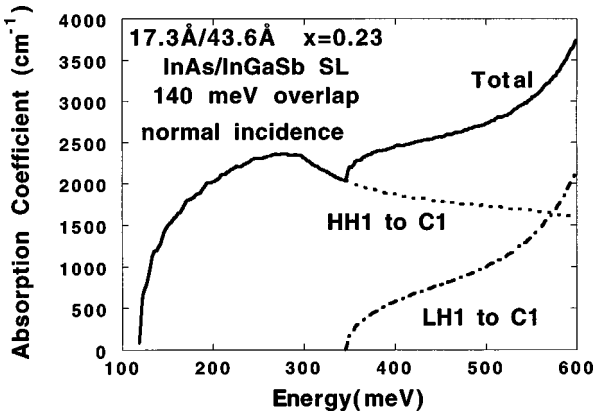

FIG. 2. The optical absorption spectrum in normal incidence for the superlattice of Fig. 1.

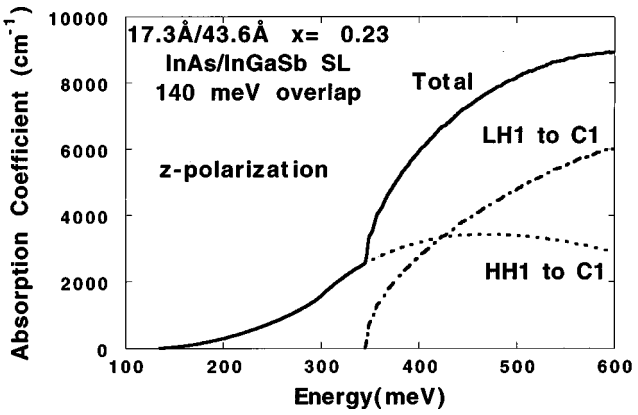

FIG. 3. The optical absorption spectrum in z polarization for the superlattice of Fig. 1.

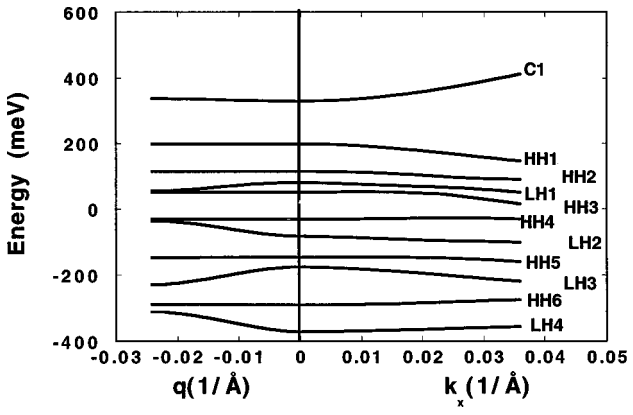

FIG. 4. The band diagram for the 38/29/63 Å $InAs/In_{0.3}Ga_{0.7}Sb/GaSb$ superlattice.

as the result of HH-LH band coupling. A complete discussion of the optical response of these structures is deferred to a future publication.

A. $InAs/In_{0.3}Ga_{0.7}Sb/GaSb$ superlattice

To demonstrate the three-layer formalism, the electronic structure of a 38/29/63 Å $InAs/In_{0.3}Ga_{0.7}Sb/InAs$ superlattice, which is of interest for infrared laser applications,[19] was calculated. To this end, Eq. (41) was used to calculate the energies as well as the wave functions in conjunction with the 8×8 EFA Hamiltonian and the standard EFA boundary conditions, as above. The structural parameters for the superlattice correspond to those used by Yang *et al.*[19] for their type-II infrared cascade laser, except that two thin AlSb layers between the InAs and $In_{0.3}Ga_{0.7}Sb$ and InAs and GaSb layers were eliminated for reasons that will become clear later. The three-layer code was tested in the two-layer limit by setting one of the layer thicknesses to zero or by having two layers have the same material composition; in this limit, the results of the three-layer code invariably agreed to within the machine accuracy with the corresponding results of the two-layer code of Sec III A. In evaluating the determinant, the secular matrix was diagonalized and roots were identified by monitoring the change in the sign of the smallest diagonal element. Typically, its magnitude did not exceed 10^{-1}.

Figure 4 shows the calculated band dispersions for the three-layer superlattice. Because of the large repeat period (130 Å), the band dispersions in the direction of the superlattice axis are rather flat. Once the energies are found, the wave functions in all three layers simultaneously can be found from the eigenvector in Eq. (41). Using the calculated wave functions, the band character of the levels at the center of the Brillouin zone was determined. Table I summarizes the wave-function decomposition of the three most important levels for the laser structure: $C1$, HH1, and HH2. In this structure, electrons are injected electrically into $C1$, from where they deexcite into HH1 by emitting a photon. The efficiency of this process depends on the overlap between the wave functions for the two levels. According to Table I, 14.2% of the $C1$ wave function is in the $In_{0.3}Ga_{0.7}Sb$ layer, which should ensure strong oscillator strength for the $C1$-to-HH1 transition.

According to the present calculation, the onset of lasing for the 38/29/63 Å $InAs/In_{0.3}Ga_{0.7}Sb/InAs$ superlattice should equal the $C1$-HH1 energy level separation of 131 meV (9.5 μm). In actual operation, the device is biased so that the long-wavelength threshold is blueshifted. In addition, the use of AlSb interlayers by Yang *et al.*[19] produces a stronger confinement of carriers in both the InAs and $In_{0.3}Ga_{0.7}Sb$ layers, which further blueshifts the threshold. However, Table I indicates that one can obtain good confinement of electrons and holes in InAs and $In_{0.3}Ga_{0.7}Sb$ layers, respectively, while retaining a strong $C1$/HH1 overlap, which guarantees strong spatially-indirect optical transitions.

TABLE I. The band decomposition by layer of the HH2, HH1, and $C1$ levels at the center of the Brillouin zone in a 38/29/63 Å $InAs/In_{0.3}Ga_{0.7}Sb/GaSb$ superlattice.

	HH2 113.21 meV	HH1 198.04 meV	$C1$ 329.18 meV
InAs C like	0	0	0.561
InAs HH like	0.006	0.010	0
InAs LH like	0	0	0.119
$In_{0.3}Ga_{0.7}Sb$ C like	0	0	0.050
$In_{0.3}Ga_{0.7}Sb$ HH like	0.076	0.823	0
$In_{0.3}Ga_{0.7}Sb$ LH like	0	0	0.092
GaSb C like	0	0	0.055
GaSb HH like	0.918	0.167	0.0
GaSb LH like	0	0	0.095

The HH2 level serves as an efficient sink[19] of electrons from the HH1 level, which deexcite from HH1 to HH2 by phonon emission, in the process creating a population inversion between levels $C1$ and HH1. Table I shows that 16.7% of the wave function for the HH1 level is in the GaSb layer, which should promote a strong coupling of the HH1 to HH2 levels. Once in the GaSb layer, the electron is sequentially injected into the next InAs/$In_{0.3}Ga_{0.7}$Sb/GaSb period.[19]

This calculation demonstrates the utility of the present formalism for three-layer superlattices. The numerical stability of the formalism was achieved at the price of an enlarged size of the secular equation. For a limited number of layers per superlattice period, this should represent an acceptable trade off.

CONCLUSIONS

The transfer-matrix approach employing Burt's boundary conditions was used to derive the tangents-only form of the secular equation for superlattices within the envelope-function approximation. This form is numerically stable and Hermitian, and it separates Kramers' degenerate solutions. The formalism is extended to any number of layers per superlattice period. The present results are directly applicable to the calculation of the electronic, elastic, optical, and magnetic properties of superlattices. The formalism was applied to the calculation of the electronic structure and the optical absorption spectrum of InAs/$In_{0.23}Ga_{0.77}$Sb superlattices for infrared detector applications. The results show strong absorption in normal incidence as well as in z polarization away from the threshold. The three-layer calculation for the infrared cascade laser structure comprised of an InAs/$In_{0.3}Ga_{0.7}$Sb/InAs superlattice demonstrates the utility of the present formalism for multilayer calculations and the design of laser devices.

ACKNOWLEDGMENTS

This work was performed under Air Force Contract No. F33615-95-C-5445 at the Materials Laboratory, Wright-Patterson Air Force Base, Ohio. The author would like to thank Dr. Thomas Vaughan and Dr. Darryl L. Smith for helpful discussions.

*Also at the University of Dayton Research Institute, Dayton, Ohio 45469-0178.

[1] G. Bastard, *Wave Mechanics Applied to Semiconductor Heterostructures* (Wiley, New York, 1988); G. Bastard, J. A. Brum, and R. Ferreira, in *Solid State Physics: Semiconductor Heterostructures, and Nanostructures*, edited by H. Ehrenreich and D. Turnbull, Solid State Physics, Vol. 44 (Academic, New York, 1991).

[2] D. M. Wood and A. Zunger, Phys. Rev. B **53**, 7949 (1996).

[3] L.-W. Wang and A. Zunger, Phys. Rev. B **54**, 11 417 (1996).

[4] M. G. Burt, J. Phys.: Condens. Matter **4**, 6651 (1992); Semicond. Sci. Technol. **3**, 739 (1988); Phys. Rev. B **50**, 7518 (1994) and references therein.

[5] B. A. Foreman, Phys. Rev. B **48**, 4964 (1993); **52**, 12 241 (1995).

[6] L. R. Ram-Mohan, K. H. Yoo, and R. L. Aggarwal, Phys. Rev. B **38**, 6151 (1988).

[7] D. L. Smith and C. Mailhiot, Phys. Rev. B **33**, 8345 (1986).

[8] F. Szmulowicz, Phys. Rev. B **54**, 11 539 (1996).

[9] A. M. Cohen and G. E. Marques, Phys. Rev. B **41**, 10 608 (1990).

[10] The similarity transformation connecting the RYA and SZ formalism is given by $\Omega_{\mathrm{RYA}}=Q\Omega_{\mathrm{SZ}}Q^{-1}$, where

$$Q^{-1}=\begin{pmatrix} I & 0 \\ -iH_2^{-1}H_1/2 & H_2^{-1} \end{pmatrix}, \quad Q=\begin{pmatrix} I & 0 \\ iH_1/2 & H_2 \end{pmatrix},$$

so that $QP_{\mathrm{SZ}}=P_{\mathrm{RYA}}$ and $f_{\mathrm{RYA}}=Qf_{\mathrm{SZ}}$.

[11] For example, in the effective-mass approximation for a three-layer ABC superlattice with layer widths $(2a,2b,2c)$, Eq. (27) gives

$$\cos qw=C_AC_BC_C+\eta_{AB}S_AS_BC_C+\eta_{BC}C_AS_BS_C+\eta_{AC}S_AC_BS_C,$$

where

$$C_A\equiv\cos 2k_Aa, \quad S_A\equiv\sin 2k_Aa, \quad \eta_{AB}\equiv\frac{m_Ak_B}{m_Bk_A}+\frac{m_Bk_A}{m_Ak_B},$$

and

$$k_A=\sqrt{2m_A(E-V_A)/\hbar^2}, \text{ etc.}$$

[12] E. Merzbacher, *Quantum Mechanics*, 2nd ed. (Wiley, New York, 1970), p. 323; also, one has $(1+i\tan\Lambda a)^{-1}=\cos^2\Lambda a[1-i\tan\Lambda a]$.

[13] For example, in the effective-mass approximation for a two-layer superlattice, Eq. (37) leads to equation $D_{\mathrm{SZ}}=(A^++\alpha B)(A^-+B/\alpha)+(A^-+\alpha B)(A^++B/\alpha)=0$, where $A^{\pm}=\tan(k_Aa\pm qd/2)$, $B=\tan k_Bb$, and $\alpha=m_Ak_B/m_Bk_A$; Also see F. Szmulowicz, Eur. J. Phys. **18**, 392 (1997); and Am. J. Phys. **65**, 1009 (1997).

[14] D. L. Smith and C. Mailhiot, J. Appl. Phys. **62**, 2545 (1987); Surf. Sci. **196**, 683 (1988); Rev. Mod. Phys. **62**, 173 (1990); C. Mailhiot and D. L. Smith, J. Vac. Sci. Technol. A **7**, 445 (1989); and R. H. Miles and D. H. Chow, in *Long Wavelength Infrared Detectors*, edited by M. Razeghi, Optoelectronic Properties of Semiconductors and Superlattices, Vol. 1, edited by M. O. Manasreh (Gordon and Breach, Amsterdam, 1996), pp. 397–452, and references therein.

[15] E. R. Heller, K. Fisher, F. Szmulowicz, and F. L. Madarasz, J. Appl. Phys. **77**, 5739 (1995); F. Szmulowicz, E. R. Heller, K. Fisher, and F. L. Madarasz, Superlattices Microstruct. **17**, 373 (1995); *Numerical Data and Functional Relationships in Science and Technology*, edited by O. Madelung, Landolt-Börnstein, New Series, Group III, Vol. 17, Pts. a–b (Springer, New York, 1982); Chris G. Van de Walle, Phys. Rev. B **39**, 1871 (1989).

[16] F. Szmulowicz, Phys. Rev. B **51**, 1613 (1995); Pis'ma Zh. Eksp. Teor. Fiz. **60**, 731 (1994) [JETP Lett. **60**, 751 (1994)].

[17] Y.-C. Chang and R. B. James, Phys. Rev. B **39**, 12 672 (1989).

[18] G. Gilat and L. J. Raubenheimer, Phys. Rev. **144**, 390 (1966); **147**, 670(E) (1966).

[19] R. Q. Yang, C.-H. L. Lin, S. J. Murry, S. S. Pei, H. C. Liu, M. Buchanan, and E. Dupont, Appl. Phys. Lett. **70**, 2013 (1997).